Hachenberg and C. Göttlinger for competent technical help, W. Müller for the method of detecting NP-specific mIgG1-positive cells, R. C. Rickert and A. Tarakhovsky for critical reading of the manuscript, and U. Ringeisen for graphical work. Supported by fellowships from the Human Frontier Science Programme (HFSP) and the Alexander von Humboldt Foundation to T.K. and by grants from the Deutsche Forschungsgemeinschaft through SFB 243, the HFSP, and the Land Nordrhein-Westfalen. F.S. was supported by a stipend of the Boehringer Ingelheim Fonds.

22 November 1996; accepted 10 February 1997

Solution Structure of 3-Oxo-Δ^5-Steroid Isomerase

Zheng Rong Wu, Soheila Ebrahimian, Michael E. Zawrotny, Lora D. Thornburg, Gabriela C. Perez-Alvarado, Paul Brothers, Ralph M. Pollack,* Michael F. Summers*

The three-dimensional structure of the enzyme 3-oxo-Δ^5-steroid isomerase (E.C. 5.3.3.1), a 28-kilodalton symmetrical dimer, was solved by multidimensional heteronuclear magnetic resonance spectroscopy. The two independently folded monomers pack together by means of extensive hydrophobic and electrostatic interactions. Each monomer comprises three α helices and a six-strand mixed β-pleated sheet arranged to form a deep hydrophobic cavity. Catalytically important residues Tyr^{14} (general acid) and Asp^{38} (general base) are located near the bottom of the cavity and positioned as expected from mechanistic hypotheses. An unexpected acid group (Asp^{99}) is also located in the active site adjacent to Tyr^{14}, and kinetic and binding studies of the Asp^{99} to Ala mutant demonstrate that Asp^{99} contributes to catalysis by stabilizing the intermediate.

Various biological reactions proceed by enzymatic cleavage of a C-H bond adjacent to a carbonyl or carboxyl group, leading to an enol or enolate intermediate that is subsequently reprotonated at the same or an adjacent carbon (*1*). Thermodynamic and kinetic barriers associated with these processes can be very large, requiring the enzymes to provide up to 20 kcal/mol of transition state stabilization (*2*). An important member of this class of enzymes is 3-oxo-Δ^5-steroid isomerase (Δ^5-3-ketosteroid isomerase, KSI, E.C. 5.3.3.1), which is among the most proficient enzymes known (*3*) and has served as a paradigm for enzymatic enolizations since its discovery in 1955 (*4*). This enzyme catalyzes the isomerization of various β,γ-unsaturated 3-oxosteroids to their conjugated isomers at nearly a diffusion-controlled rate (*5*).

Extensive kinetic and mutagenesis studies indicate that catalysis proceeds by predominant abstraction of the steroid C4-β proton by Asp^{38}, with stabilization of the resulting dienolate intermediate by a hydrogen bond from Tyr^{14}-OH (*6–10*). Nuclear magnetic resonance (NMR) studies have led to the conclusion that the intermediate is stabilized by a single low barrier hydrogen bond (LBHB) (*11*), and it has been further proposed that the entire rate enhancement by KSI can be quantitatively attributed to residues Asp^{38} and Tyr^{14} (*11*). Nevertheless, fluorescence titration of the Tyr^{14}-OH suggests the presence of an active site residue with pK_a of 9.5 (*12*), and there is evidence that this unknown group is catalytically important (*13, 14*). There is also a substantial contribution to the rate of enzymatic proton transfer by Phe^{101} that has yet to be satisfactorily explained (*15*).

Despite more than 20 years of effort, high-resolution structural information that would identify all of the active site residues and facilitate a complete mechanistic analysis has been lacking. Crystals of KSI that diffract to 2.7 Å have been reported (*16, 17*), and a three-dimensional (3D) model refined to 6 Å resolution suggested that the substrate binding site is located within a cavity near the dimer interface (*18*). In order to provide a more detailed and independent assessment of the solution structure of KSI, we have determined its complete 3D structure using heteronuclear multidimensional and triple resonance NMR methods.

^{15}N- and $^{15}N,^{13}C$-labeled KSI samples for NMR studies were expressed in *Escherichia coli* and purified under nondenaturing conditions (*19*). Protein aggregation is significant at dimer concentrations greater than 80 μM (*20*), and was inhibited when 90% water and 10% dioxane-d_8 were used as solvent. The introduction of dioxane led to small chemical shift changes (<0.1 ppm) for only a few NMR signals, and to a minor reduction in enzyme activity (*21*), indicating that the protein structure was not significantly altered under these conditions. Gradient-enhanced triple-resonance NMR methods, including four-dimensional $^{15}N,^{13}C$- and $^{13}C,^{13}C$-edited nuclear Overhauser effect (NOE) experiments, were used to assign the backbone and side chain signals (*22*). The observation of 117 of the 119 expected backbone NH correlation signals per polypeptide in the NMR spectra revealed that the protein dimer is structurally symmetric. Intermolecular NOEs were identified by comparing the four-dimensional (4D) NOE NMR data obtained for the uniformly labeled dimer with 3D pulsed-field gradient-edited ^{13}C-filtered–^{12}C-detected NOE data obtained for a heterodimer comprising nonlabeled and $^{15}N,^{13}C$-labeled subunits. For example, the Val^{74}-γ^2CH_3 exhibits intramolecular NOE cross peaks with Val^{74}-γ^1CH_3, -Hβ, -Hα (Fig. 1A), as well as intermolecular cross peaks with Leu^{115}-Hα, -Hγ, -δ^2CH_3 and with Val^{40}-Hβ and -CH_3 protons (Fig. 1B). With this approach, we were able to unambiguously assign 30 intermolecular NOE cross peaks.

A total of 1865 experimental distance restraints identified from the NOE data were used to generate an ensemble of 20 distance geometry structures with the program DIANA (*23*). Statistical information

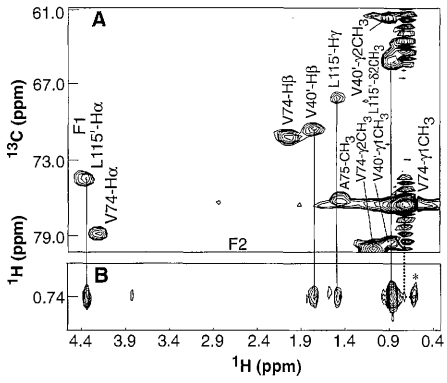

Fig. 1. Nuclear Overhauser effect (NOE) data associated with the Val_{74}-γ^2CH_3 methyl group. (**A**) Selected plane [F4 (^1H) = 0.74 ppm; F3 (13C) = 16.48 ppm] from the 4D $^{13}C,^{13}C$-edited NOE spectrum showing both intermolecular (denoted with primes) and intramolecular dipolar interactions. (**B**) Corresponding plane from the 3D gradient-purged ^{13}C-filtered–^{12}C-detected half-filtered NOE spectrum [F1 (^{13}C) = 16.48 ppm] showing intermolecular NOE correlation signals (* denotes the incompletely suppressed Val^{74}-γ^2CH_3 autopeak doublet).

Z. R. Wu, M. E. Zawrotny, G. C. Perez-Alvarado, M. F. Summers, Howard Hughes Medical Institute and Department of Chemistry and Biochemistry, University of Maryland Baltimore County, 1000 Hilltop Circle, Baltimore, MD 21250.
S. Ebrahimian, L. D. Thornburg, P. Brothers, R. M. Pollack, Department of Chemistry and Biochemistry, University of Maryland Baltimore County, 1000 Hilltop Circle, Baltimore, MD 21250, and Center for Advanced Research in Biotechnology (R. M. Pollack), 9600 Gudelsky Drive, Rockville, MD 20850.
*To whom correspondence should be addressed.

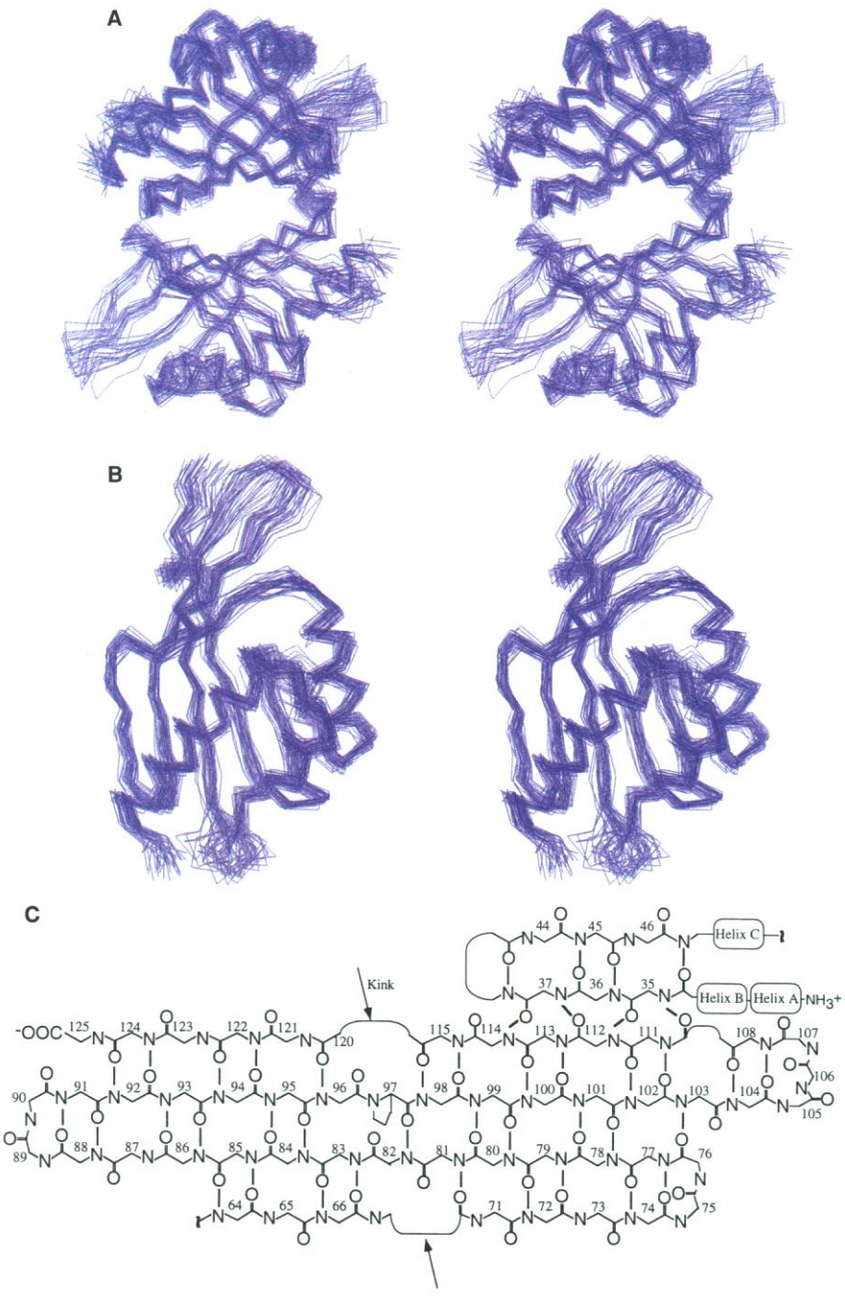

Fig. 2. (**A**) Stereoview showing the best fit superposition of the backbone Cα atoms of 20 distance-geometry models of the KSI-dimer generated with DIANA (*23*). Higher convergence is observed when the superposition is performed for the monomeric subunits (**B**) resulting from a small amount of disorder at the dimer interface (Table 1). (**C**) Schematic diagram showing the secondary structure of the KSI β sheet. The β sheet contains a significant kink along the axis denoted by arrows. (**D**) Ribbon representation of KSI with the independent subunits colored red and green, showing the "back-to-back" packing and relationship between the subunits.

for the structure calculations (Table 1) and stereo views of the best fit superposition of the backbone atoms for the dimer and the monomeric subunits (Figs. 2, A and B) demonstrate that the calculations afford a single globular protein fold with good convergence. The structure is composed of three α helices and a six-strand mixed β-pleated sheet that contains three β bulges (Fig. 2C). Residues that make up these secondary structure elements are as follows: Thr^{3} (the NH_2-terminal helix capping residue, N-cap) to Ala^{20} form helix A; Asp^{22} (N-cap) to Phe^{30} form helix B; Ala^{34} to Asp^{38} form strand 1 of the six-strand β sheet; cis-Pro^{39} (which contains a cis-peptidyl linkage) to Ser^{42} form a four-residue loop; Glu^{43} to Gly^{47} form strand 2 of the β sheet, which runs antiparallel to strand 1; Thr^{48} to Leu^{61} form helix C; and Leu^{63} to Gly^{124} form the remaining four strands of the six-strand mixed β sheet as follows. Leu^{63} to Val^{74} form strand 3, with Thr^{68} to Glu^{70} forming a β bulge; Ala^{75} to Asn^{76} form a type II turn; Glu^{77} to Tyr^{88} form strand 4, which runs antiparallel to strand 3; Gln^{89} to Gly^{90} form a type II turn; Arg^{91} to Phe^{104} form strand 5, which runs antiparallel to strand 4; Asn^{105}-Val^{107} form a loop; Lys^{108} to Gly^{124} form strand 6, which contains two

Table 1. Structural statistics

Distance restraints	
Intraresidue	49
Sequential	306
Medium range ($\|i–j\|$ = 2–5 residues)	351
Long range ($\|i–j\|$ > 5 residues)	545
Intermolecular	60
Hydrogen bond restraints	554
Total NMR-derived restraints	1865
Mean restraints/residue	15.2
Distance violations	
Total penalty (Å^2)	
Mean	0.75 ± 0.16
Maximum	0.97
Minimum	0.45
Individual violation (Å)	
Maximum	0.20
Average maximum	0.16 ± 0.03
Average number of violations >0.1 Å per structure	4 ± 2
Pairwise root-mean-square (Å)	
Monomer backbone heavy atoms	
α helices*	0.65 ± 0.16
β sheet + β bulges†	0.92 ± 0.20
Met^1 to Ala^{125}	1.24 ± 0.19
Dimer backbone heavy atoms	
α helices‡	1.06 ± 0.24
β sheet + β bulge§	1.19 ± 0.22
Met^1 to ^{125}Ala	1.54 ± 0.24

*Residues 3–20, 22–30, 48–61. †Residues 34–38, 43–47, 63–74, 77–88, 91–103, 111–124. ‡Residues 3–20, 22–30, 48–61, 3′–20′, 22′–30′, 48′–61′ (unprimed and primed numbers refer to the different monomers). §Residues, 34–38, 43–47, 63–74, 77–88, 91–103, 111–124, 34′–38′, 43′–47′, 63′–74′, 77′–88′, 91′–103′, 111′–124′.

β bulges (Val[109] to Val[110] and Phe[116] to Asn[120]) and runs antiparallel to strand 5 and parallel to strand 1.

The β sheet contains a substantial kink that appears to result from the juxtapositioning of two β bulges at opposite edges of the sheet with a proline residue (Pro[97]) located in the center of the sheet and between the bulges (Fig. 2C). Strands 3 and 4 of the β sheet make extensive hydrophobic contacts with helix A, which also packs tightly against helix B. Helix B is packed between helices A and C and is arranged nearly antiparallel to both. Helices B and C cross over the "front face" of the β sheet, forming a hydrophobic cavity with approximate dimensions 8.5 Å by 9.5 Å at the surface and 16 Å deep. One side of the cavity is lined with residues from the "front face" of the β sheet, including hydrophobic residues Val[36], Pro[39], Leu[63], Val[65], Leu[67], Val[71], Phe[80], Phe[82], Val[84], Val[95], Pro[97], Phe[101], Ala[114], and Phe[116], as well as acidic residues Asp[38] and Asp[99]. The other side of this cavity is composed of residues that reside on the α helices, including Val[11], Tyr[14], Val[15], Leu[18], Phe[54], and Tyr[55]. The two monomers of the symmetrical dimer pack against each other via hydrophobic and electrostatic interactions that exclusively involve the side chains of residues on the "back face" of the β sheet (Fig. 2D). There are no main chain hydrogen bonds between the monomers. This global structure and, in particular, the dimer interface, appear distinctly different from that of the low resolution x-ray structure (*18*).

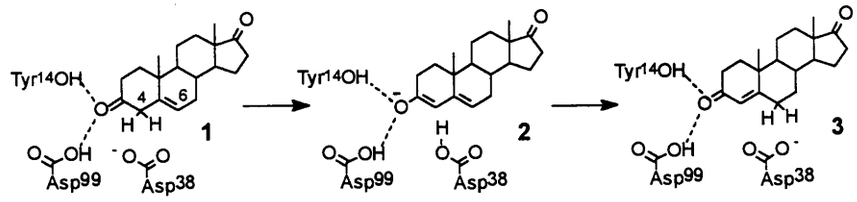

Scheme 1

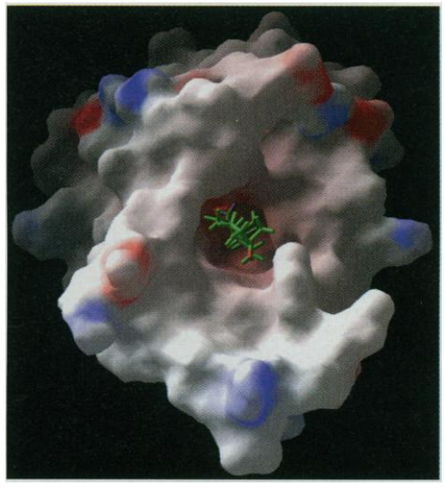

Fig. 3. Surface representation of KSI, colored according to electrostatic potential, showing the acidic nature of the active site cavity. A substrate molecule (5-androstene-3,17-dione) docked computationally in an orientation consistent with the postulated mechanism and experimental NMR data (*25*) is also shown in a ball-and-stick representation. The docking of the substrate molecule did not require reorientation of the protein amino acid side chains.

To evaluate the proposal that Asp[38] and Tyr[14] function as the general base and general acid, respectively (*6*, *7*), a substrate molecule (5-androstene-3,17-dione, *1*) was docked computationally into the active site [X-PLOR (*24*)] with the H2α,β protons in close proximity to Tyr[14]-Hε, which is consistent with previous NMR data (*25*), and with the carbonyl oxygen within hydrogen bonding distance of Tyr[14]-OH (*6*, *26*). Protein conformational changes were not required to perform this docking (Fig. 3). In the resulting model, one of the carboxyl oxygens of Asp[38] is located 2.8 Å above the 4β proton, in excellent position to abstract this proton with the *syn* orbitals of the carboxylate (*27*) (Scheme 1). Subsequent rotation about the Cβ-COOH bond places the carboxyl proton directly above the steroid C6 carbon, enabling proton transfer to C6 of the dienolate intermediate. The structure is thus entirely compatible with the previously proposed mechanistic roles of Asp[38] and Tyr[14].

An additional acid residue (Asp[99]) is located near the back of the active site cavity in close proximity to Asp[38] and Tyr[14]. The Asp[99] carboxyl group is also ~3 Å from the 3-carbonyl of the docked substrate, suggesting that the acid could play an important role in stabilizing the intermediate and transition states. To test this hypothesis, we prepared the D99A (*28*) mutant and found that it was substantially less active than the wild-type enzyme (k_{cat} and k_{cat}/K_m are ~5000 and ~3000 times lower, respectively) (*29*), confirming the importance of Asp[99] to catalysis. This mutant exhibits a decrease in affinity (30 times lower) for the intermediate analog equilenin (*30*), comparable to the ~10-fold decrease in affinity of the Y14F mutant for the intermediate analog estradiol (*6*). These results indicate that both Tyr[14] and Asp[99] stabilize the reaction intermediate, and that their energetic contributions are similar in magnitude.

We propose that the dienolate intermediate is stabilized by two hydrogen bonds, one from Tyr[14]-OH and the other from Asp[99]-COOH (Scheme 1). In this model, residue Asp[99] is protonated in the enzyme-intermediate complex, which is reasonable given the close proximity of Asp[99] to Asp[38] in the low-dielectric environment of the active site cavity (*31*). Stabilization by protonated Asp[99] is consistent with the observed diminution of catalytic activity at high pH, which has been attributed to ionization of an unknown active site group with a pK_a of about 9.5 (*13*, *14*). This group, which is not Tyr[14] or Tyr[55] (*12*), is likely Asp[99], the only other ionizable residue within the active site other than the catalytic general base Asp[38]. Thus, the kinetics, mutagenesis, pH titration, inhibitor binding, and structural data are consistent with a COOH–intermediate hydrogen bonding role for Asp[99]. Although Asp[99] could form a hydrogen bond to the Tyr[14] oxygen, our proposal that the intermediate is stabilized by two hydrogen bonds (from Asp[99] and Tyr[14]), rather than a single LBHB (*11*, *32*), is consistent with the suggestion that enzymes use multiple interactions of moderate strength as a catalytic strategy (*33*). Two hydrogen bonds of moderate strength (about 4 to 5 kcal/mol), along with the contribution of Phe[101] (2 kcal/mol), would be sufficient to account for the observed (*5*) 11 kcal/mol stabilization of the bound dienolate ion intermediate.

REFERENCES AND NOTES

1. J. A. Gerlt, J. W. Kozarich, G. L. Kenyon, P. G. Gassman, *J. Am. Chem. Soc.* **113**, 9667 (1991).
2. S. Shan, S. Loh, D. Herschlag, *Science* **272**, 97 (1996).
3. A. Radzicka and R. Wolfenden, *ibid.* **267**, 90 (1995).
4. P. Talalay and V. S. Wang, *Biochim. Biophys. Acta* **18**, 300 (1955).
5. D. C. Hawkinson, T. C. M. Eames, R. M. Pollack, *Biochemistry* **30**, 10849 (1991).
6. A. Kuliopulos, A. S. Mildvan, D. Shortle, P. Talalay, *ibid.* **28**, 149 (1989).
7. W. F. Benisek, J. R. Ogez, S. B. Smith, *Ann. N.Y. Acad. Sci.* **346**, 115 (1980).
8. P. L. Bounds and R. M. Pollack, *Biochemistry* **26**, 2263 (1987).
9. M. E. Zawrotny, D. C. Hawkinson, G. Blotny, R. M. Pollack, *ibid.* **35**, 6438 (1996).
10. A. Viger, S. Coustal, A. Marquet, *J. Am. Chem. Soc.* **103**, 451 (1981).
11. Q. Zhao, C. Abeygunawardana, P. Talalay, A. S. Mildvan, *Proc. Natl. Acad. Sci. U.S.A.* **93**, 8220 (1996).
12. Y.-K. Li, A. Kuliopulos, A. S. Mildvan, P. Talalay, *Biochemistry* **32**, 1816 (1993).
13. H. Weintraub, A. Alfsen, E.-E. Baulieu, *Eur. J. Biochem.* **12**, 217 (1970).
14. C. M. Holman and W. F. Benisek, *Biochemistry* **34**, 14245 (1995).
15. P. N. Brothers, G. Blotny, L. Qi, R. M. Pollack, *ibid.*, p. 15453.

16. E. M. Westbrook, *J. Mol. Biol.* **103**, 659 (1976).
17. E. M. Westbrook *et al., ibid.*, p. 665.
18. E. M. Westbrook, O. E. Piro, P. B. Sigler, *J. Biol. Chem.* **259**, 9096 (1984).
19. KSI was expressed in *E. coli* strain NCM533, supplied by M. C. Betlach [R. F. Shand, L. J. W. Miercke, A. K. Mitra, S. K. Fong, R. M. Stroud, M. C. Betlach, *Biochemistry* **30**, 3082 (1991)]; we used M9 minimal medium containing either $^{15}NH_4Cl$ or $^{15}NH_4Cl$ and [^{13}C]glucose [J. Sambrook, E. F. Fritsch, T. Maniatis, *Molecular Cloning: A Laboratory Manual* (Cold Spring Harbor Laboratory Press, Cold Spring Harbor, NY, ed. 2, 1989)] and supplemented with vitamins [R. A. Venters, T. L. Calderone, L. D. Spicer, C. A. Fierke, *Biochemistry* **30**, 4491 (1991)] and trace elements (10 μM each of $FeCl_3$, $CaSO_4$, $MnSO_4$ and $ZnSO_4$). The protein was purified as described [M. E. Zawrotny and R. M. Pollack, *Biochemistry* **33**, 13896 (1994)]. The amino acid sequence of KSI is: M^1-N-T-P-E-H-M-T-A-V^{10}-V-Q-R-Y-V-A-A-L-N-A^{20}-G-D-L-D-G-I-V-A-L-F^{30}-A-D-D-A-T-V-E-D-P-V^{40}-G-S-E-P-R-S-G-T-A-A^{50}-I-R-E-F-Y-A-N-S-L-K^{60}-L-P-L-A-V-E-L-T-Q-E^{70}-V-R-A-V-A-N-E-A-A-F^{80}-A-F-T-V-S-F-E-Y-Q-G^{90}-R-K-T-V-V-A-P-I-D-H^{100}-F-R-F-N-G-A-G-K-V-V^{110}-S-M-R-A-L-F-G-E-K-N^{120}-I-H-A-G-A^{125} [A. Kuliopulos, D. Shortle, P. Talalay, *Proc. Natl. Acad. Sci. U.S.A.* **84**, 8893 (1987); K. Y. Choi, W. F. Benisek, *Gene* **69**, 121 (1988)].
20. W. F. Tivol, E. D. Beckman, W. F. Benisek, *J. Biol. Chem.* **250**, 271 (1975).
21. A 20% decrease in k_{cat} is accompanied by an increase in K_m (five times), as is expected for this change in solvent composition [F. Falcoz-Kelly, E.-E. Baulieu, A. Alfsen, *Biochemistry* **7**, 4119 (1968)]. The near independence of k_{cat} on solvent composition is consistent with a lack of a structural perturbation.
22. NMR data were collected with Bruker DMX and GE Omega PSG 600 MHz (^{1}H) spectrometers for KSI samples (1 mM dimer) in D_2O or 90% H_2O and 10% D_2O containing 10 mM phosphate buffer (pH 7.0), and 10% dioxane-d_8. NMR data were processed with Felix™ (Molecular Simulations, Inc.) or NMRPipe [F. Delaglio, S. Grzesiek, G. W. Vuister, G. Zhu, J. Pfeifer, A. Bax, *J. Biomol. NMR* **6**, 277 (1995)] and analyzed with NMRVIEW [B. A. Johnson and R. A. Blevins, *ibid.* **4**, 603 (1994)]. Water signal suppression was achieved with the use of flip-back pulses [S. Grzesiek and A. Bax, *J. Am. Chem. Soc.* **115**, 12593 (1993)], pulsed field gradients [M. Piotto, V. Saudek, V. Sklenar, *J. Biomol. NMR* **2**, 661 (1992)], or presaturation pulses during the relaxation delay. Signal assignments were made from 3D HNCA and HN(CO)CA data [S. Grzesiek and A. Bax, *J. Magn. Reson.* **96**, 432 (1992)], 3D HCCH-COSY [M. Ikura, L. E. Kay, A. Bax, *J. Biomol. NMR* **1**, 299 (1991)], 3D HCCH-TOCSY [A. Bax, G. M. Clore, A. M. Gronenborn, *J. Magn. Reson.* **88**, 425 (1990)], and 3D ^{15}N-edited TOCSY data [X. Y. Marion *et al., Biochemistry* **28**, 6150 (1989)] obtained with a 75-msec clean-MLEV-17 mixing period [C. Griesinger, G. Otting, K. Wüthrich, R. R. Ernst, *J. Am. Chem. Soc.* **110**, 7870 (1988)] and sensitivity-improved gradient coherence selection [O. Zhang, L. E. Kay, J. P. Olivier, J. D. Forman-Kay, *J. Biomol. NMR* **4**, 845 (1994)]. NOE data (τ_m = 100 msec) were obtained from 2D NOESY [J. Jeener, B. H. Meier, P. Bachmann, R. R. Ernst, *J. Chem. Phys.* **71**, 4546 (1979); S. Macura and R. R. Ernst, *Mol. Phys.* **41**, 95 (1980)], 3D ^{15}N-edited NOESY-HSQC [X. Y. Marion *et al., Biochemistry* **28**, 6150 (1989)] and 3D ^{13}C-edited HMQC-NOESY data [S. W. Fesik and E. R. P. Zuiderweg, *J. Magn. Reson.* **78**, 588 (1988)]. Intermolecular NOEs were identified from double half-filtered ^{13}C NOESY data [M. Ikura and A. Bax, *J. Am. Chem. Soc.* **114**, 2433 (1992); W. Lee, M. J. Revington, C. Arrowsmith, L. E. Kay, *FEBS Lett.* **350**, 87 (1994)].
23. P. Güntert, W. Braun, K. Wüthrich, *J. Mol. Biol.* **217**, 517 (1991); P. Güntert and K. Wüthrich, *J. Biomol. NMR* **1**, 447 (1991). Secondary structural elements were identified by analysis of NOE cross-peak patterns [K. Wüthrich, *NMR of Proteins and Nucleic Acids* (Wiley, New York, 1986)] and ^{13}Cα chemical shift indices [S. Spera and A. Bax, *J. Am. Chem. Soc.*, **113**, 5490 (1991); D. S. Wishart, B. D. Sykes, F. M. Richards, *J. Mol. Biol.* **222**, 311 (1991); D. S. Wishart, B. D. Sykes, F. M. Richards, *Biochemistry* **31**, 1647 (1992); D. S. Wishart and B. D. Sykes, *J. Biomol. NMR* **4**, 171 (1994)]. Only functional restraints were included in the calculations (for example, in cases where a proton exhibited NOEs of different intensities to geminal methylene protons, restraints were only employed for the stronger of the two cross peaks). Color figures were generated with Midas-plus [T. E. Ferrin, C. C. Huang, L. E. Jarvis, R. Langridge, *J. Mol. Graph.* **6**, 13 (1988)], Molscript [P. J. Kraulis, *J. Appl. Crystallogr.* **24**, 946 (1991)], and Raster-3D [D. J. Bacon and W. F. Anderson, *J. Mol. Graphics* **6**, 219 (1988)].
24. A. T. Brünger, *X-PLOR: A System for X-ray Crystallography and NMR* (Yale Univ. Press, New Haven, ed. 3.1, 1993).
25. A. Kuliopulos, G. P. Mullen, L. Xue, A. S. Mildvan, *Biochemistry* **30**, 3169 (1991).
26. D. C. Hawkinson and R. M. Pollack, *ibid.* **32**, 694 (1993).
27. R. D. Gandour, *Bioorg. Chem.* **10**, 169 (1981).
28. Single letter abbreviations for the amino acids are: A, Ala; D, Asp; E, Glu; F, Phe; G, Gly; H, His; I, Ile; K, Lys; L, Leu; M, Met; N, Asn; P, Pro; Q, Gln; R, Arg; S, Ser; T, Thr; V, Val; and Y, Tyr.
29. Oligonucleotide-directed mutagenesis was performed according to the method of Eckstein and coworkers [J. R. Sayers, C. Krekel, F. Eckstein, *BioTechniques* **13**, 592 (1992)]. The D99A protein was expressed in DH5α *E. coli* (grown in LB medium and induced with isopropyl-β-thiogalactopyranoside), and purified as described above (*19*). The resulting protein was homogeneous, on the basis of SDS-PAGE. Steady-state kinetic constants for the reaction of D99A with 5-androstene-3,17-dione (*1*) were determined in 34 mM phosphate, pH 7.0, 3.3% methanol as previously described for wild-type enzyme [R. M. Pollack, S. Bantia, P. L. Bounds, B. M. Koffman, *Biochemistry* **25**, 1905 (1986)].
30. Fluorescence titration of equilenin with D99A was carried out in 10 mM potassium phosphate buffer, pH 7.0, with 3.3% methanol, and gave a value for K_D of 67 ± 37 μM, compared to a K_D of 2 μM for wild-type enzyme [D. C. Hawkinson, R. M. Pollack, N. P. Ambulos Jr., *Biochemistry* **33**, 12172 (1994)]. Equilenin was also tested as an inhibitor of the D99A reaction with 5-androstene-3,17-dione under first-order conditions [R. M. Pollack, R. H. Kayser, C. L. Bevins, *Biochem. Biophys. Res. Commun.* **91**, 783 (1979)], and was found to have a K_i of >100 μM.
31. A high p*K*a (>9) has been observed for a buried aspartic acid in reduced thioredoxin [N. A. Wilson, E. Barbar, K. Langsetmo, J. A. Fuchs, C. Woodward, *Biochemistry* **34**, 8931 (1995)].
32. A highly deshielded ^{1}H NMR signal (18.15 ppm) has been observed for complexes between KSI mutants and the intermediate-analogs dihydroequilenin and estradiol-17β-hemisuccinate (*11*). This signal was absent in spectra obtained for complexes with a KSI mutant that lacks Tyr^{14}, and was attributed to the Tyr^{14}-OH proton in a LBHB with an energy of >7 kcal/mol. We observe a similar 17.4 ppm signal for a wild-type KSI-equilenin complex, which disappears upon substitution of Asp^{99} by Ala. Further experiments are thus required to identify the origin of the downfield-shifted signal.
33. S. Shan and D. Herschlag, *J. Am. Chem. Soc.* **118**, 5515 (1996).
34. Supported by NIH grants GM38155 and GM49082. We thank M. C. Betlach for supplying us with the *E. coli* strain NCM933, and M. R. Starich for technical assistance and for collecting some of the NMR data. Coordinates and NMR restraints have been deposited in the Brookhaven Protein Data Bank with accession numbers 1ISK and R1ISKMR, respectively.

12 December 1996; accepted 2 February 1997

The Product of the Proto-Oncogene c-*cbl*: A Negative Regulator of the Syk Tyrosine Kinase

Yasuo Ota and Lawrence E. Samelson*

Engagement of antigen and immunoglobulin receptors on hematopoietic cells is directly coupled to activation of nonreceptor protein tyrosine kinases (PTKs) that then phosphorylate critical intracellular substrates. In mast cells stimulated through the FcεRI receptor, activation of several PTKs including Syk leads to degranulation and release of such mediators of the allergic response as histamine and serotonin. Regulation of Syk function occurred through interaction with the Cbl protein, itself a PTK substrate in this system. Overexpression of Cbl led to inhibition of Syk and suppression of serotonin release from mast cells, demonstrating its ability to inhibit a nonreceptor tyrosine kinase. Complex adaptor proteins such as Cbl can directly regulate the functions of the proteins they bind.

Cbl, the product of the proto-oncogene c-*cbl*, is a prominent substrate of the cellular PTKs activated by multiple immune and growth factor receptors (*1*, *2*). Both the retroviral gag-v-cbl fusion protein and a Cbl protein containing a 17–amino acid internal deletion, which was isolated from the 70Z pre–B cell tumor line, are transforming in fibroblast and pre–B cells (*3*). However, the function of the proto-oncogene product remains undefined. The fact that it undergoes tyrosine phosphorylation and that it binds critical signaling molecules such as PTKs and adaptor molecules such as Grb2 and the phosphoinositide-3 kinase subunit p85, and the observation that SLI-1, a *Caenorhabditis elegans* homolog, has an inhibitory effect on the Ras pathway suggest that Cbl has a critical function in signal transduction (*4*). Cbl is rapidly tyrosine phosphorylated in the rat basophilic leukemia cell line RBL-2H3 after antigen-induced aggregation of the FcεRI receptor (*5*). In

Cell Biology and Metabolism Branch, National Institute of Child Health and Human Development, National Institutes of Health, Bethesda, MD 20892–5430, USA.

*To whom correspondence should be addressed. E-mail: samelson@helix.nih.gov